

Measurement of electric potential fields

Matthew Krupcale, Oliver Ernst

Department of Physics, Case Western Reserve University, Cleveland Ohio, 44106-7079

18 November 2012

Abstract

In electrostatics, Laplace's equation can be used with appropriate boundary conditions to find the potential in a region free of charge or with steady current. The electric potential for four separate two-dimensional configurations of conductors was measured in a homogenous, conductive medium and compared to the theoretical solution. A numerical relaxation method was also used to compare the measured potential. In the regions where the theoretical models were valid, the measured potentials were within one to two deviations of the theoretical potential uncertainties for each configuration. The numerical solutions had large deviations around areas of sharp changes in potential and had relative errors of 10 to 100 percent of the measured potential in many regions. The analytic models can be further adjusted to account for limitations in the physical configuration, and the numerical methods can be further optimized to handle both large and small features of the configuration.

Introduction

The electric potential fields were measured for a parallel plate capacitor, cylindrical capacitor, infinite plane with a line charge image and parallel plates with an insulator inserted. In regions where the potential can be analytically solved (ignoring edge effects), the theory was compared to the measured values in each configuration. Additionally, a numerical relaxation method was used with the corresponding boundary conditions to compare the numerical solutions of Laplace's equation to the measured potential. Qualitative and quantitative

comparisons of the theoretical or numerical values and the actual measurements were made using surface and contour plots.

Theory

In a region of steady current, the continuity equation implies that the current density is divergenceless, $\nabla \cdot \mathbf{J} = 0$. Thus, for a homogenous material that satisfies Ohm's law, the electric field is also divergenceless [1]. So the electric potential satisfies Laplace's equation in a homogenous material carrying a steady current [2]:

$$\nabla^2 V = 0 \quad (1)$$

Solutions to Laplace's equation can be found using techniques of separation of variables, symmetry arguments and other special techniques like the method of images. See the Appendix for the details of deriving these solutions.

Parallel Plate Capacitor

The infinite parallel plate capacitor is a well-known problem in electrostatics that can be solved exactly due to symmetry arguments. Suppose that the plates are parallel to the planes defined by $y = \pm \frac{a}{2}$, where a is the separation between the plates. Then the potential depends only on y and has the solution to Laplace's equation

$$V(y) = \left(\frac{V_0 - V_1}{a}\right)y + \frac{1}{2}(V_0 + V_1) \quad (2a)$$

where V_2 and V_1 are the potentials of the lower and upper plates, respectively. We can ground the lower plate so $V_1 = 0$, and the solution becomes

$$V(y) = \left(\frac{V_0}{a}\right)y + \frac{V_0}{2} \quad (2b)$$

Cylindrical Capacitor

The cylindrical or coaxial capacitor consists of two concentric cylindrical conductors of radii $R_0 < R_1$ for the inner and outer cylinders, respectively. The inner conductor is held at

potential V_0 , and the outer conductor is held at potential V_1 . Due to the cylindrical symmetry, the potential is independent of the azimuthal angle and depends only on the radial distance from the central axis. The solution in all regions is given by

$$V(r) = \begin{cases} V_0, r < R_0 \\ \frac{V_0 \ln R_1 - V_1 \ln R_0}{\ln\left(\frac{R_1}{R_0}\right)} + \frac{V_0 - V_1}{\ln\left(\frac{R_0}{R_1}\right)} \ln r, R_0 < r < R_1 \\ V_1, r > R_1 \end{cases} \quad (3a)$$

where $r = \sqrt{x^2 + y^2}$. If we ground the outer conductor so that $V_1 = 0$, this simplifies to

$$V(x, y) = \begin{cases} V_0, r < R_0 \\ \frac{V_0}{\ln\left(\frac{R_0}{R_1}\right)} \ln\left(\frac{\sqrt{x^2 + y^2}}{R_1}\right), R_0 < r < R_1 \\ 0, r > R_1 \end{cases} \quad (3b)$$

Line Charge Image

One way of finding the solution to Laplace's equation for particularly convenient geometries is to use the method of images, whereby image charges are placed outside of the volume of interest such that the boundary conditions of the original problem are satisfied. Then the potential inside the region of interest is uniquely defined and can be found using the charge distribution of real and image charges. One such geometry consists of a line charge parallel to an infinite grounded conducting plane, which has circular cylinder equipotential surfaces parallel to the line charge. Thus, defining a circular equipotential in the homogenous material at a given distance away from an infinite grounded plane is equivalent to placing an infinite line charge in the material.

Suppose that the grounded plane is the $y = 0$ plane (the xz plane), and that the circular equipotential at voltage V_0 is centered at $(0, y_0, 0)$ with radius $0 < R_0 < y_0$. The potential function that satisfies these boundary conditions and thus Laplace's equation is

$$V(x, y) = \frac{V_0}{2 \operatorname{asech}\left(\frac{R_0}{y_0}\right)} \ln \left(\frac{x^2 + \left(y + \sqrt{y_0^2 - R_0^2}\right)^2}{x^2 + \left(y - \sqrt{y_0^2 - R_0^2}\right)^2} \right) \quad (4)$$

where ϵ_0 is the vacuum permittivity.

Parallel Plates with Insulator

Removing a portion of the conducting medium is equivalent to inserting an electrical insulator in that region. Placing an insulator or a dielectric material in the conducting medium has the effect of preventing current from flowing through the region of the dielectric. Thus, current is forced to flow around the dielectric, and charges in the dielectric will tend to move opposite of the external electric field, building up at the boundary of the dielectric. The result is that there tends to be a higher potential near the positive electrode and a lower potential near the negative electrode than if there were no dielectric present. In a homogenous, linear dielectric material, the bound volumetric charge density is proportional to the free volumetric charge density, so if no charge is embedded within the material, the material obeys Laplace's equation [2]. At the boundary, however, surface charges may still exist.

Apparatus and Methods

The electric potential field for each configuration was mapped using the PASCO scientific MODEL PK-9023 Field Mapper set, which includes conductive paper, silver conductive ink pen, a corkboard surface and metallic pins. The conductive ink was drawn onto the paper and connected through the metallic pins to an Agilent E3610A power supply with a fixed potential of $V_0 = 10.025 \text{ V}$. Since the ink has nonzero resistance, the pins were arranged in a way that minimized the effects of the potential drop across the electrodes on the measurement of the potential. These effects, however, should be small since the resistance of the paper is roughly 5 to 6 orders of magnitude greater than the resistance of the ink. The electric potential

was then measured relative to the negative electrode with a Keithley Model 2000 DMM (input resistance of at least $10\text{ G}\Omega$) at relevant points on the conductive paper. The electrode configurations tested are shown in Figures 1 through 4.

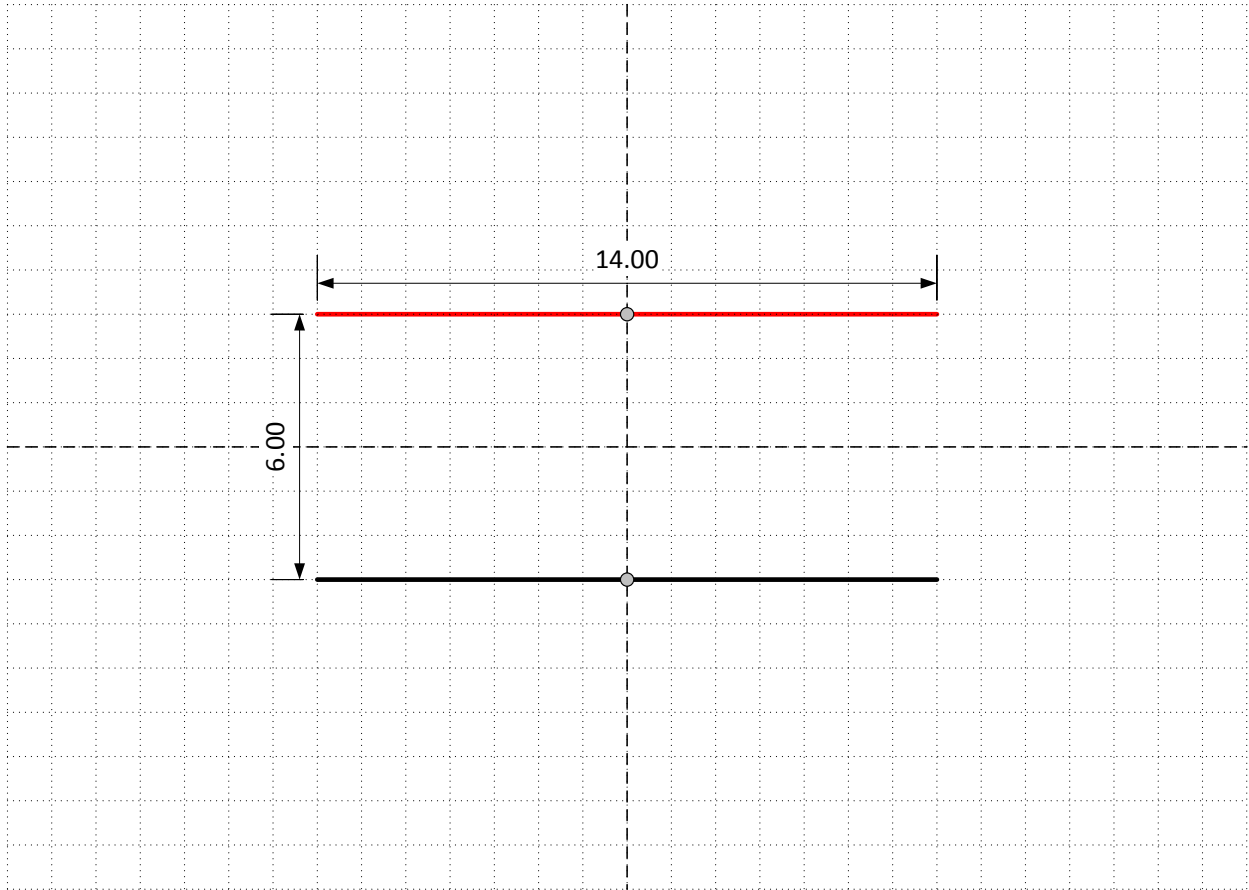


Figure 1 Parallel plate capacitor configuration. The negative electrode is shown in thick black; the positive electrode is shown in thick red. The metallic pins on the electrodes are indicated by the small silver circles. Thick dotted lines indicate symmetry axes and the xy coordinate axes, while the intersections of thin dotted lines indicate measurement points and are separated by 1 cm in both dimensions. Using symmetry, only the upper left quadrant of the parallel plate capacitor was measured, from which the rest of the measurements can be inferred.

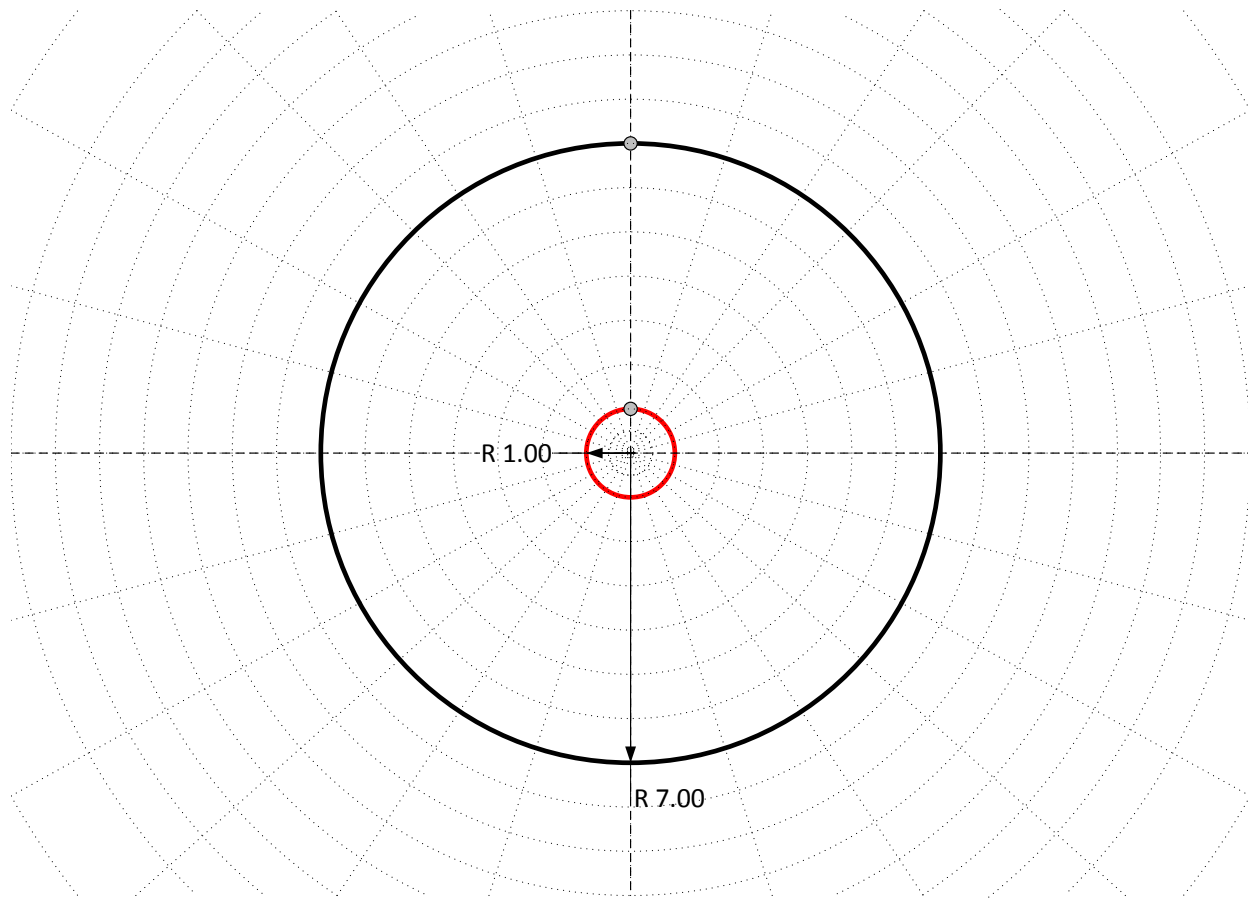


Figure 2 Cylindrical capacitor configuration. The negative electrode is shown in thick black; the positive electrode is shown in thick red. The metallic pins on the electrodes are indicated by the small silver circles. Thick dotted lines indicate symmetry axes and/or the xy coordinate axes, while the intersections of thin dotted lines indicate measurement points and are radially separated by 1 cm or in some cases 0.5 cm. Using symmetry, only the left half of the cylindrical capacitor was measured, from which the rest of the measurements can be inferred.

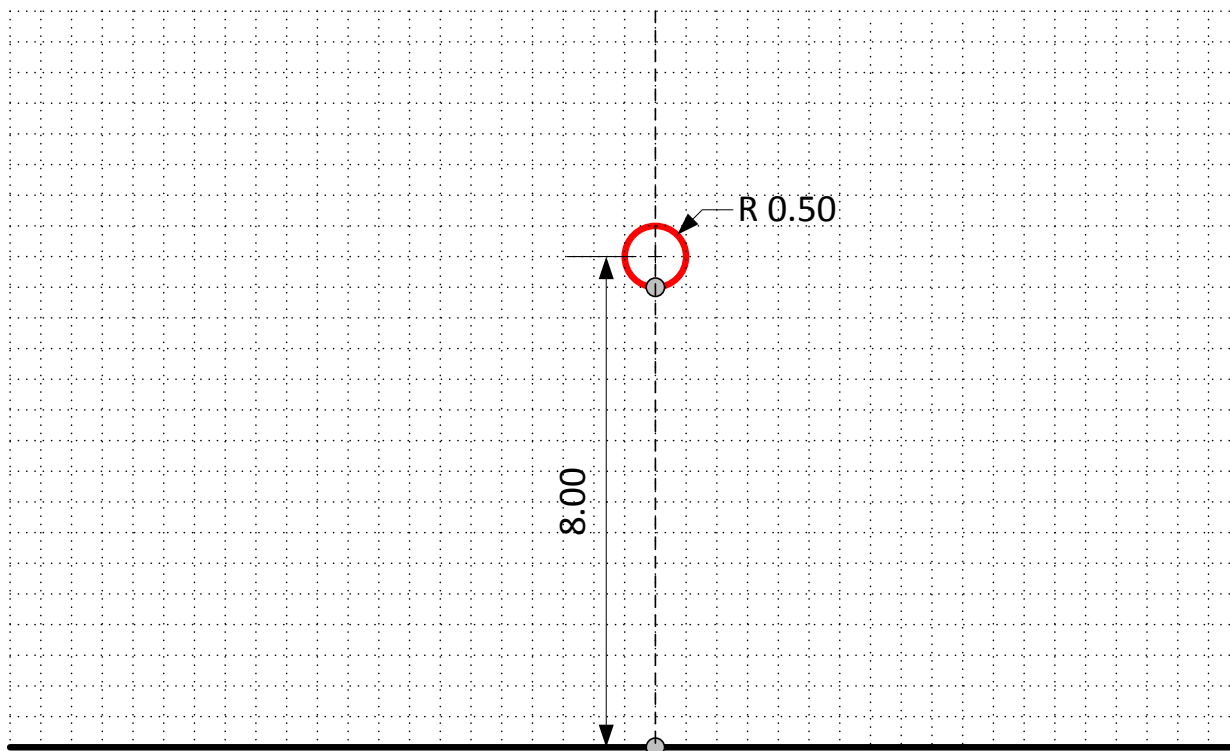


Figure 3 Line charge image configuration. The negative electrode is shown in thick black; the positive electrode is shown in thick red. The metallic pins on the electrodes are indicated by the small silver circles. Thick dotted lines indicate symmetry axes and the xy coordinate axes, while the intersections of thin dotted lines indicate measurement points and are separated by 1 cm in both dimensions.

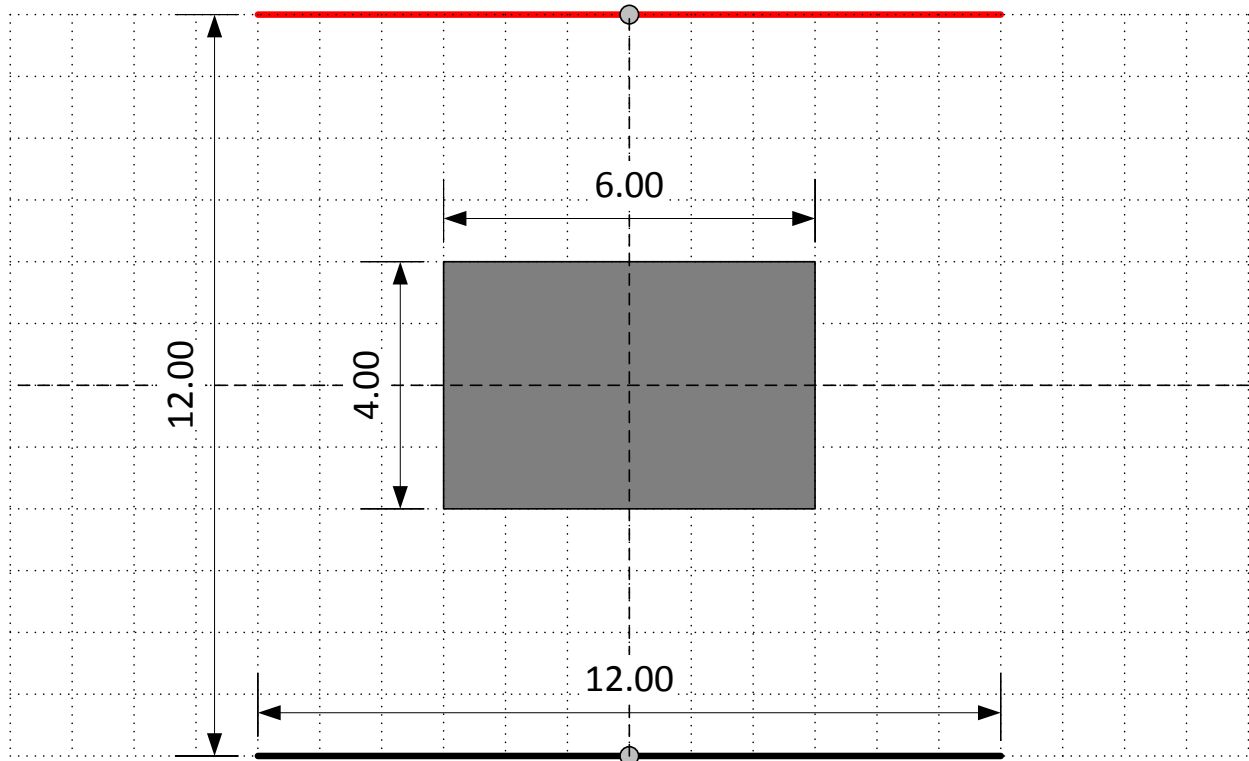


Figure 4 Insulating box configuration. The negative electrode is shown in thick black; the positive electrode is shown in thick red. The metallic pins on the electrodes are indicated by the small silver circles. Thick dotted lines indicate symmetry axes and the xy coordinate axes, while the intersections of thin dotted lines indicate measurement points and are separated by 1 cm in both dimensions. The insulator—a cut out of the conducting paper—is placed symmetrically between the plates, as shown in grey.

Results and Analysis

Two-dimensional curve fits were performed in regions where the potential could be analytically solved (ignoring edge effects) for each configuration. The fit parameters were then compared to the actual values used for each configuration. The curve fits for the cylindrical capacitor and parallel plate capacitor yielded parameter values that were close to the actual values but were either not within their uncertainties, or the uncertainties were unreasonably large. Of all configurations, the line charge configuration had the best agreement between the fit parameters and the actual values. A qualitative and quantitative comparison can be made using contour and surface plots that show the difference between measured values and theoretical values of either analytical models or numerical solutions found by finite difference methods. The

measured and numerically calculated potential fields were linearly or cubically interpolated to produce smoother surfaces for plotting.

Due to the high accuracy of the Kiethley 2000 DMM, voltage measurement uncertainties were on the order of 0.1 mV, which corresponds to roughly 10^{-5} relative uncertainty in a typical measurement. Thus, most of the uncertainty is in the theoretical model due to uncertainty in the actual geometric parameters of the configurations. The uncertainty in each distance measurement was typically 2 mm (about the width of the conductive ink), producing typical relative uncertainties in the lengths of three percent or less. However, the uncertainties in the theoretical voltage based on these parameters ranged from about 50 mV to 500 mV, and the relative uncertainties ranged from one percent up to 70 percent. Typical relative uncertainties were around 10 percent throughout most of the plane, though.

Parallel Plate Capacitor

The linear fit parameters in Eq. 2b for the region between the parallel plates were $V_0 = 9.4 \pm 0.2$ V and $a = 7.1 \pm 0.2$ cm, which are not within the uncertainty of the actual values of $V_0 = 10.025$ V and $a = 6.0$ cm. Figures 5 and 6 show the surface and contour plots of the measured potential with linear interpolation for the finite parallel plate capacitor.

Parallel Plate Capacitor Potential Surface Plot

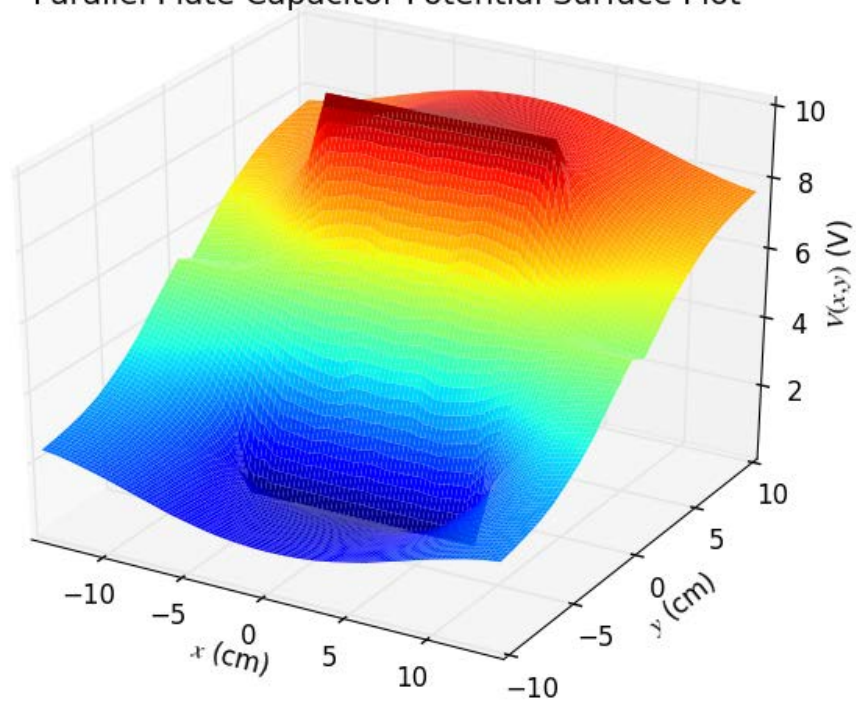


Figure 5 Finite parallel plate capacitor potential field. The parallel plates are located at the sharp ridges, with the lower plate being grounded and the upper plate held at potential $V_0 = 10.025$ V. The color (as well as the height) indicates the magnitude of the potential, with blue being small potential and red being large potential.

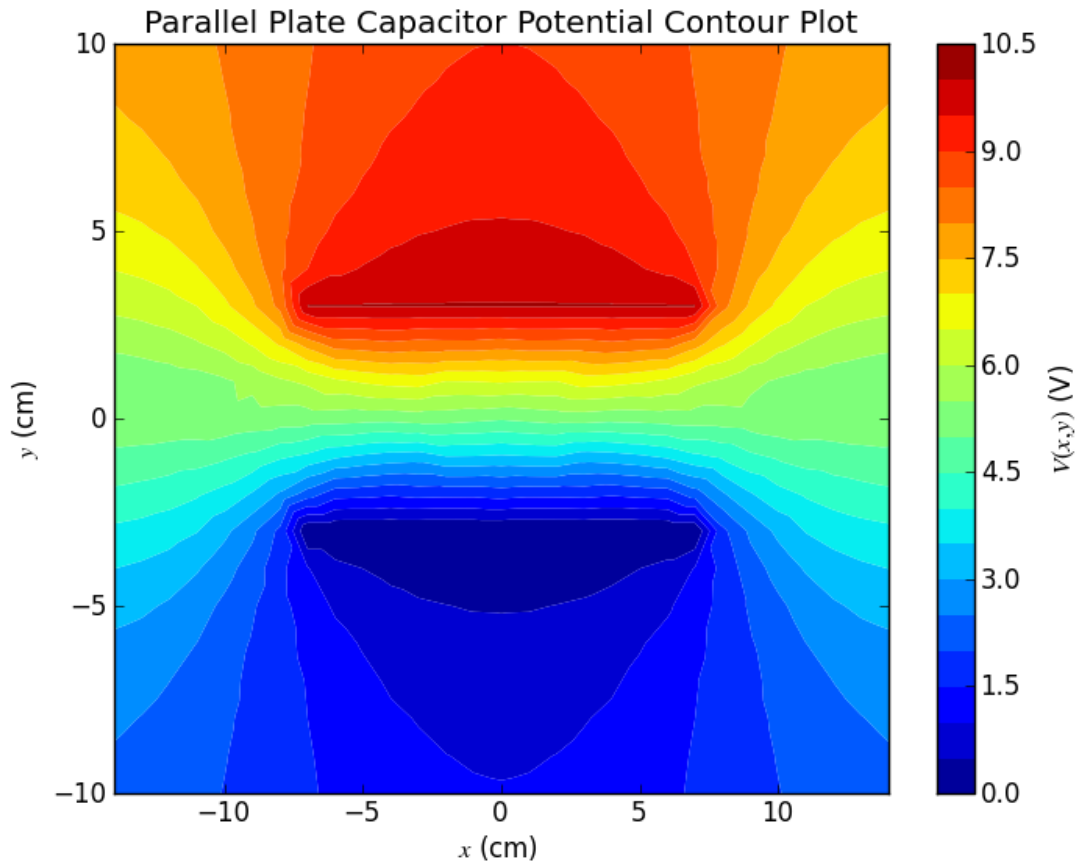


Figure 6 Contour plot for a finite parallel plate capacitor. The plates are located at $y = \pm 3$ cm from $x = -7$ cm to $x = 7$ cm. A total of 24 equipotential contour lines are plotted, with dense contours indicating rapid changes in potential.

Figure 7 shows the relative deviation between the measured potentials and the theoretical model within the plates of a parallel plate capacitor in terms of the uncertainty in the potential predicted by the model. Outside of the plates, the uncertainty with respect to the geometric parameters becomes zero, since the infinite parallel plate capacitor model predicts constant potentials inside this region. Thus, the relative deviation in this region is very large, so the absolute deviation between the measured and theoretical potentials is plotted in this region instead.

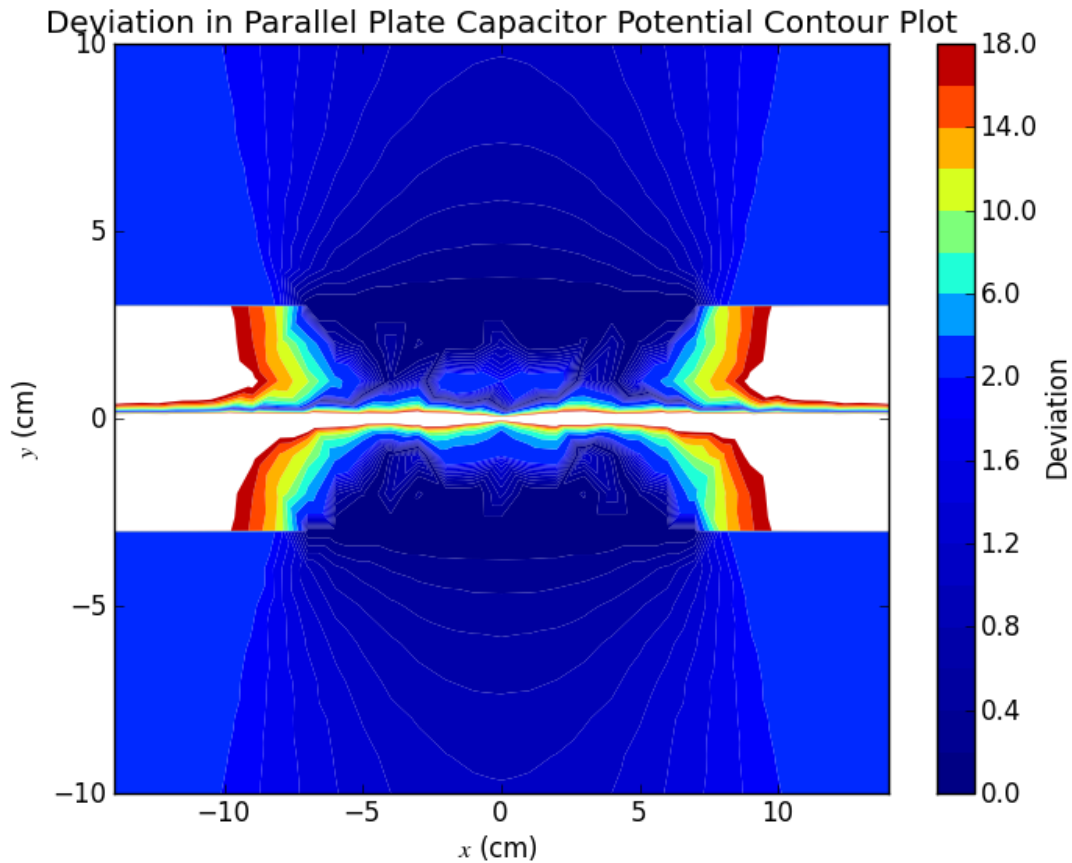


Figure 7 Relative deviation between theoretical and actual potentials for parallel plate capacitor. The units are in number of deviations relative to the uncertainty in the potential of the theoretical model. Within the plates, away from the edges ($x = \pm 7$ cm), the theoretical and measured values are usually within 2 deviations. Outside of the plates, the absolute deviation does not exceed 2 V. At $y = 0$, the relative deviation increases drastically since the uncertainty in Eq 2b. is infinitesimal at $y = 0$.

Figures 8 through 10 show the numerical solutions to Laplace's equation with the boundary conditions imposed by the parallel plates and their deviation with respect to the actual measurements. Comparing Figures 5 and 8 or 6 and 7 shows that the potential around the exterior region of the plates deviate significantly, but the region between the plates is nearly linear in the y direction, as expected from Eq 2b. More explicitly, Figure 10 shows that the deviation within the plates is on the order of 500 mV while outside it is around 3 V, corresponding to roughly 10 to 100 percent relative error.

Parallel Plate Capacitor Finite Difference Potential Surface Plot

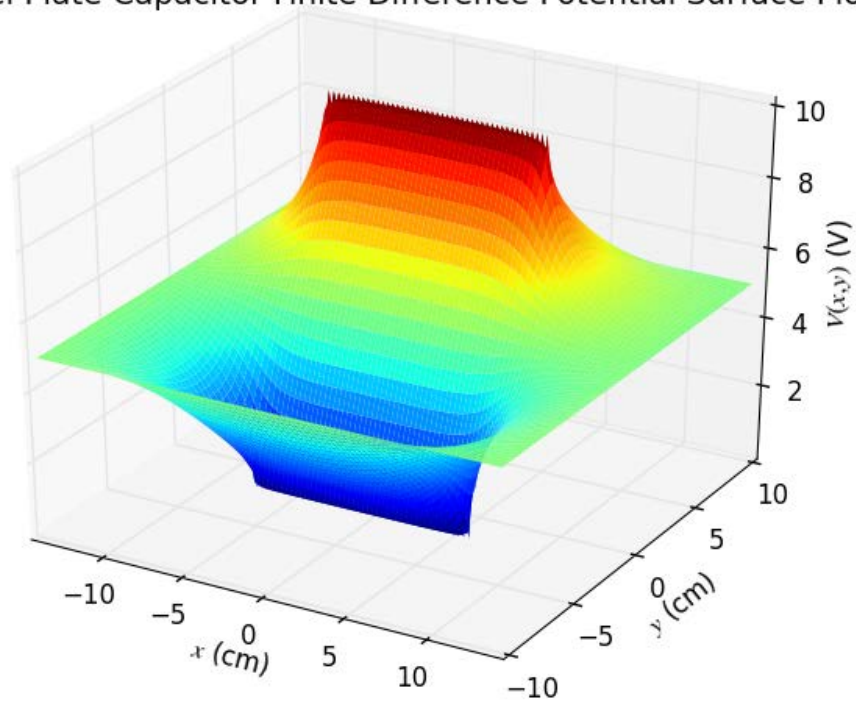


Figure 8 Surface plot of numerical solution to Laplace's equation for the parallel plate capacitor. The solution area was initialized to a potential of $\frac{V_0}{2}$ and the upper plate and lower plates were fixed at $V_0 = 10.025$ V and 0 V, respectively.

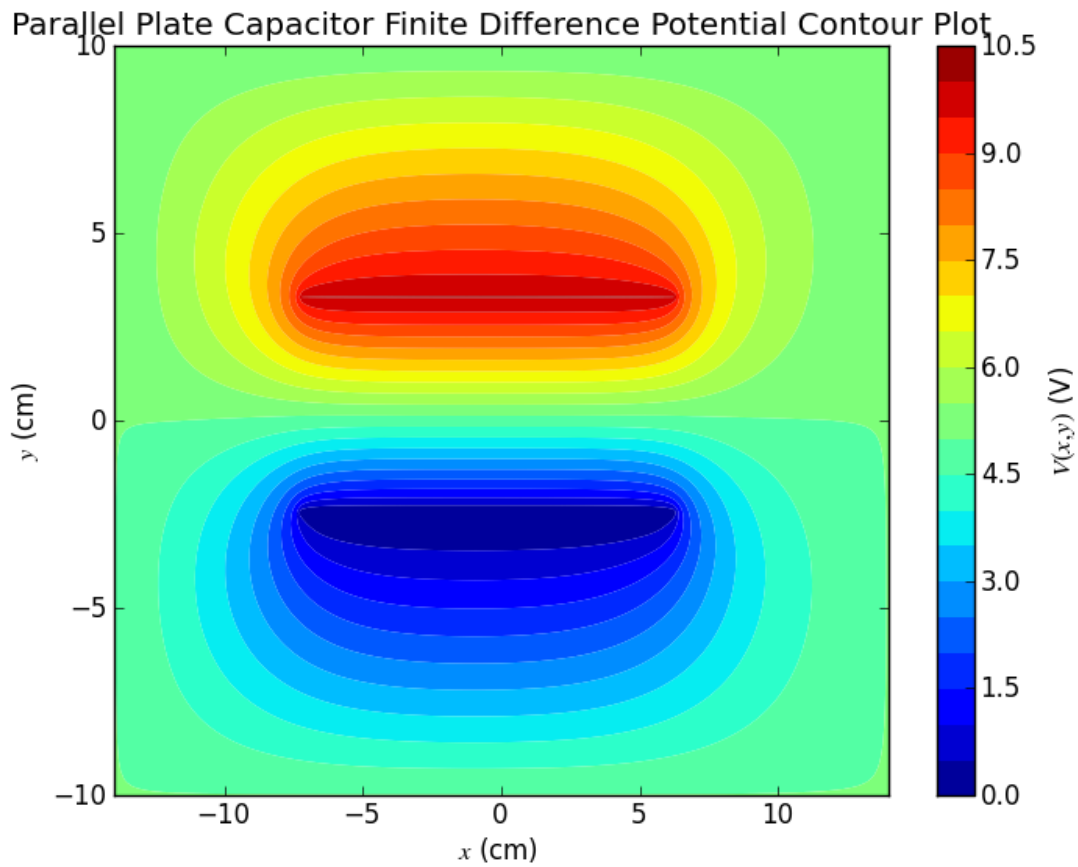


Figure 9 Contour plot of numerical solution to Laplace's equation for the parallel plate capacitor. The solution area was initialized to a potential of $\frac{V_0}{2}$ and the upper plate and lower plates were fixed at $V_0 = 10.025$ V and 0 V, respectively.

Figure 10 Absolute Deviation in Parallel Plate Capacitor Potential Contour Plot

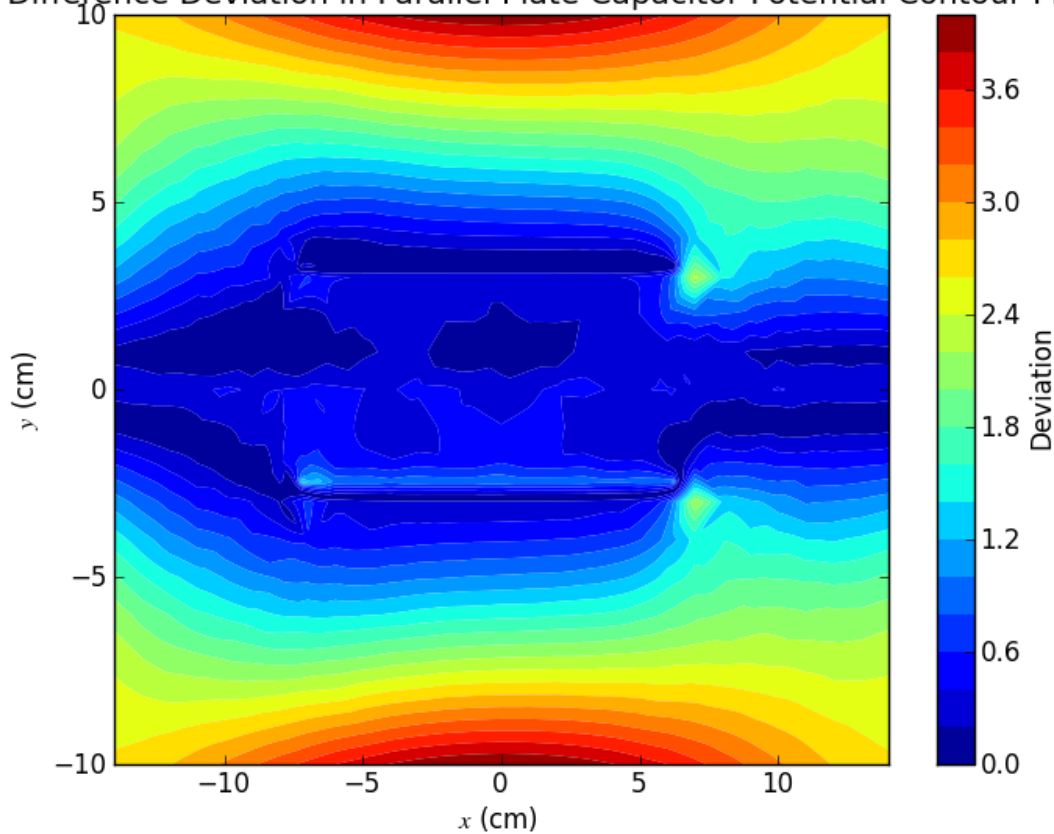


Figure 10 Absolute deviation between the numerical solution and measured potentials for the parallel plate capacitor.

Cylindrical Capacitor

In the region between the two cylinders, a curve fit to Eq. 3b produced parameters of $V_0 = 9.82 \text{ V}$, $R_0 = 1.03 \text{ cm}$ and $R_1 = 6.98 \pm 0.01 \text{ cm}$ compared to the actual values of $V_0 = 10.025 \text{ V}$, $R_0 = 1.0 \text{ cm}$ and $R_1 = 7.0 \text{ cm}$. The uncertainties in the voltage and inner radius fit parameter were on the order of 10^{13} V and 10^5 cm , respectively, which are unrealistically large. The outer radius is within two standard deviations of the actual value, and the voltage and outer radius are both within three percent relative error. The contour and surface plots of the measured potentials for the cylindrical capacitor configuration are shown in Figures 11 and 12.

Cylindrical Capacitor Potential Surface Plot

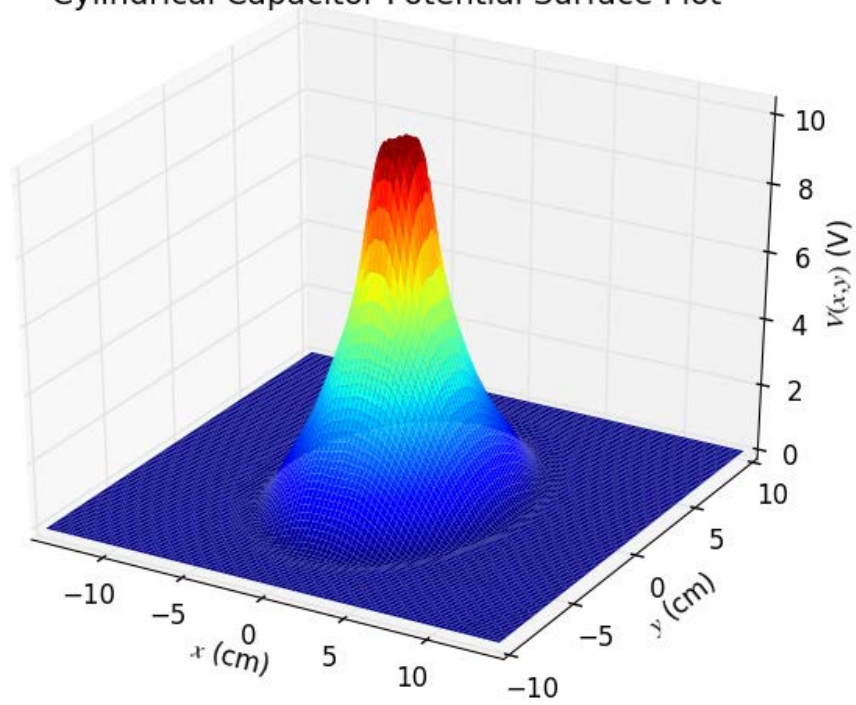


Figure 11 Cylindrical capacitor surface plot. The inner cylinder at potential $V_0 = 10.025$ V is located at the tip of the thorn-like peak, and the grounded outer cylinder is located right at its base. The color (as well as the height) indicates the magnitude of the potential, with blue being small potential and red being large potential.

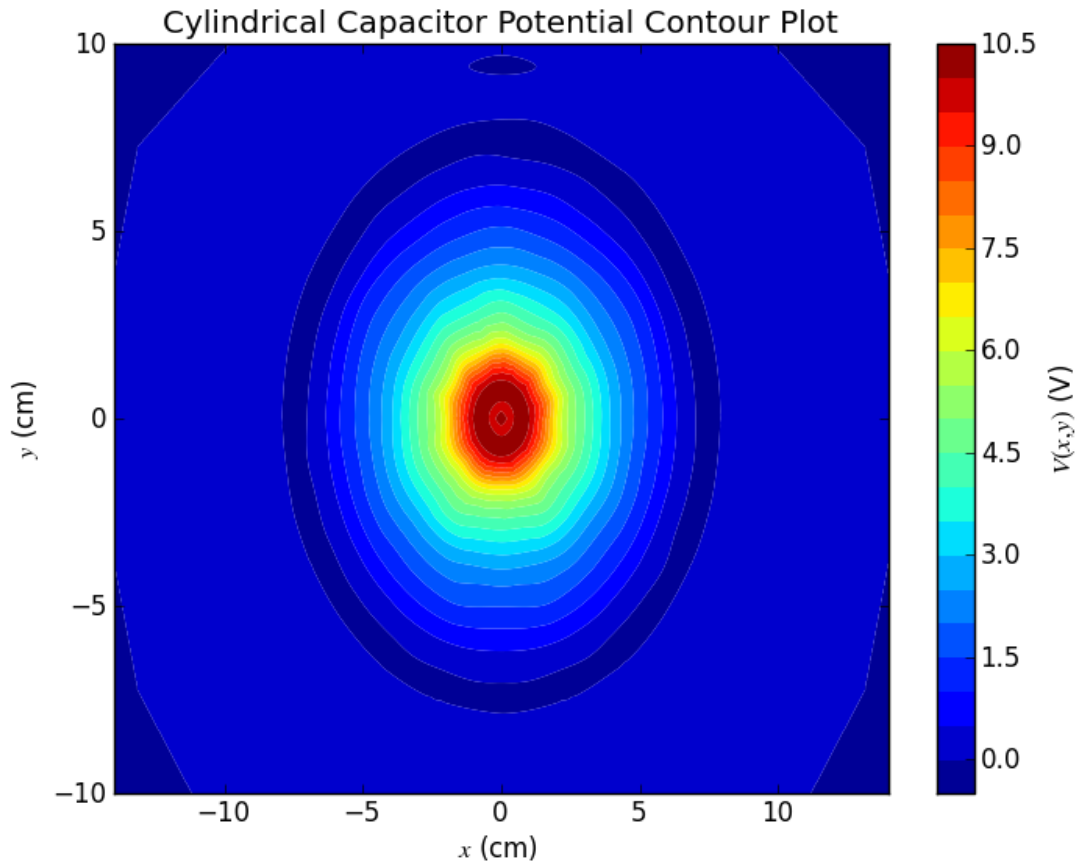


Figure 12 Contour plot for a cylindrical capacitor. The outer grounded conductor of radius $R_1 = 7$ cm is near the dark blue ring, and the inner conductor of radius $R_0 = 1$ cm is near the dark red ring. A total of 24 equipotential contour lines are plotted, with dense contours indicating rapid changes in potential.

The relative deviation between the theoretical potentials and actual potentials between the two cylinders is shown in Figure 13. Outside of this region, Eq 3b model predicts constant potentials, which corresponds to zero uncertainty with respect to the geometric parameters. Thus, in the regions exterior to the cylindrical capacitor, the absolute deviation between the theoretical and measured values is plotted (on the same scale).

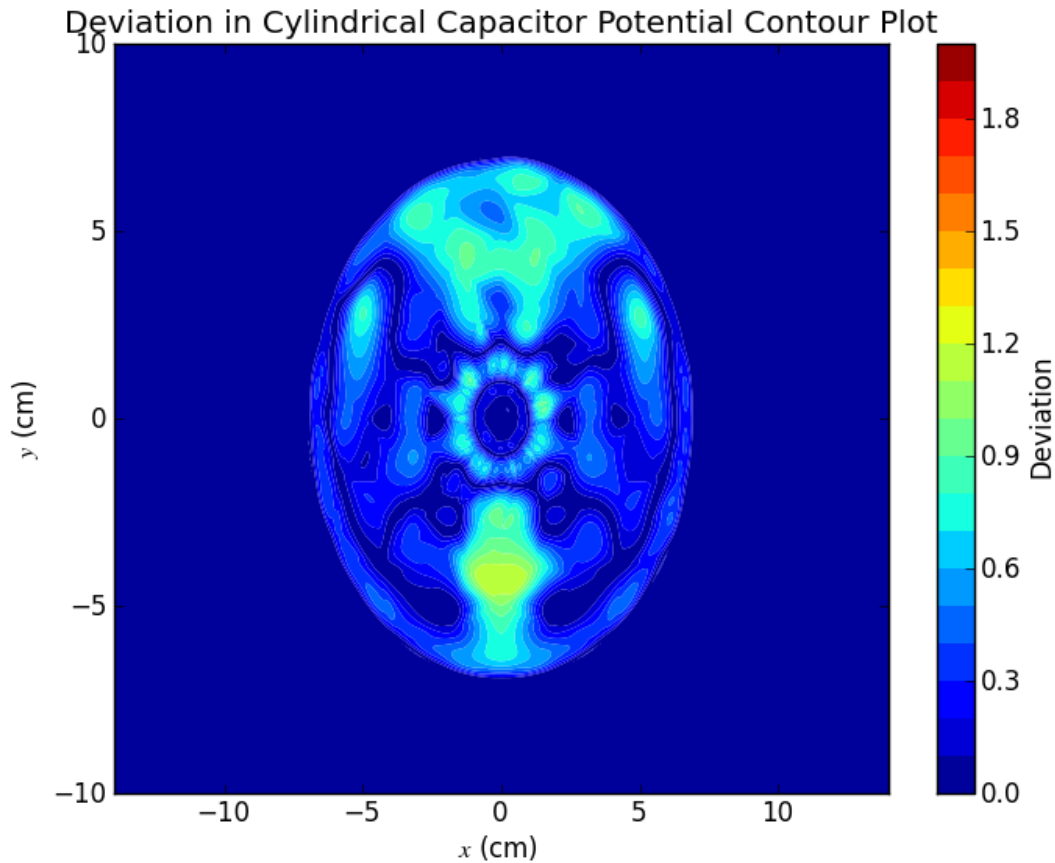


Figure 13 Relative deviation between theoretical and actual potentials for cylindrical capacitor. The units are in number of deviations relative to the uncertainty in the potential of the theoretical model. Within the cylinders of radii $R_0 = 1$ cm and $R_1 = 7$ cm, the theoretical and measured potentials are nearly always within 2 deviations. Outside of this region, the cylindrical capacitor model predicts constant potentials, resulting in large relative deviations in these regions. The absolute deviations in these regions are typically less than 0.1 V.

The numerical solution to the cylindrical capacitor potentials is shown in Figures 14 and 15, while the deviation compared to the measured potentials is shown in Figure 16. Examining Figure 16, the largest deviations are near the peak; Figure 14 shows that there are jagged outcrops in the peak, even after cubic interpolation. There is also a relatively large deviation around the outer cylinder, which is probably due to the smoothing effect that the relaxation method to solving Laplace's equation has, causing the peak to be raised more around the base.

Cylindrical Capacitor Finite Difference Potential Surface Plot

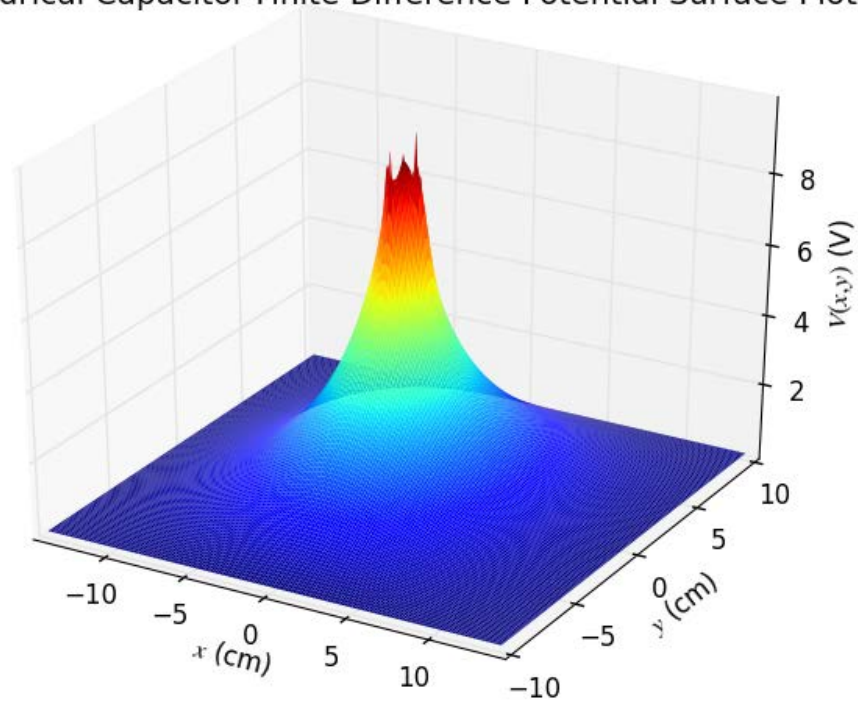


Figure 14 Surface plot of numerical solution to Laplace's equation for the cylindrical plate capacitor. The solution area was initialized to a potential of 0 V outside the capacitor, $0.5V_0$ between the cylinders and $1.1V_0$ inside the inner cylinder, where $V_0 = 10.025$ V. The inner and outer cylinders themselves were fixed at V_0 and 0, respectively.

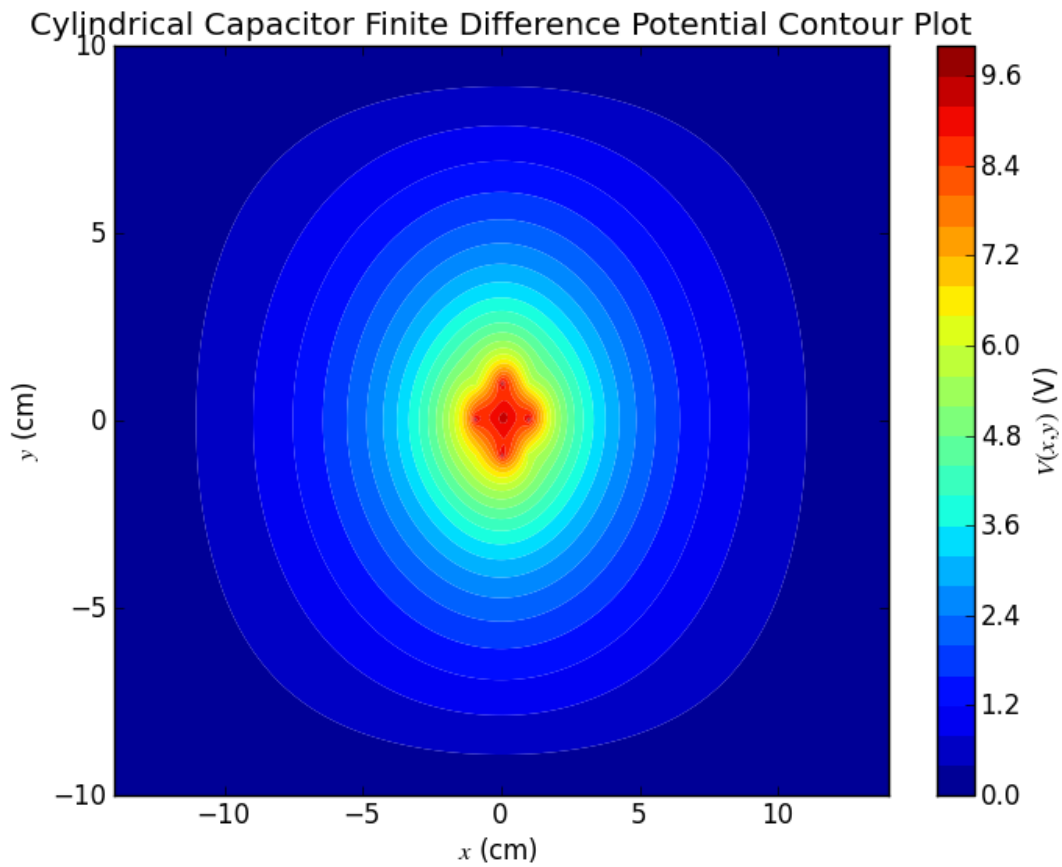


Figure 15 Contour plot of numerical solution to Laplace's equation for the cylindrical capacitor. The solution area was initialized to a potential of 0 V outside the capacitor, $0.5V_0$ between the cylinders and $1.1V_0$ inside the inner cylinder, where $V_0 = 10.025$ V. The inner and outer cylinders themselves were fixed at V_0 and 0, respectively.

Figure 16 Absolute Deviation between the numerical solution and measured potentials for the cylindrical plate capacitor.

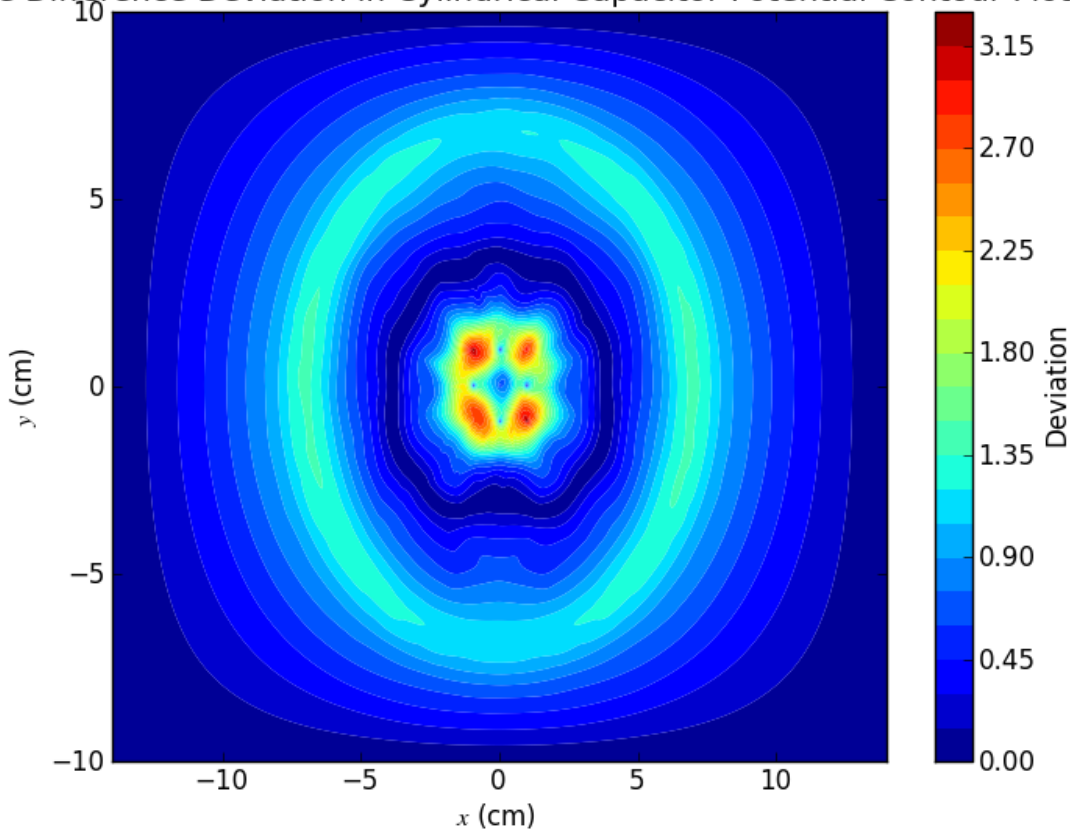


Figure 16 Absolute deviation between the numerical solution and measured potentials for the cylindrical plate capacitor.

Line Charge Image

The best fit parameters for Eq. 4 in the line charge image configuration were $V_0 = 11.8 \text{ V}$, $y_0 = 8.5 \pm 0.1 \text{ cm}$ and $R_0 = 0.53 \text{ cm}$ compared to the actual values of $V_0 = 10.025 \text{ V}$, $y_0 = 8.0 \text{ cm}$ and $R_0 = 0.5 \text{ cm}$. The relative uncertainty of the separation and radius are both about six percent. Again the uncertainties in the voltage and radius were somewhat large at 15 V and 2 cm, respectively, which would suggest (unreasonably) that the voltage and radius could have been negative. Figures 17 and 18 show the potential surface and contour plots of the line charge image configuration. Figure 19 shows the relative deviation for the line charge image.

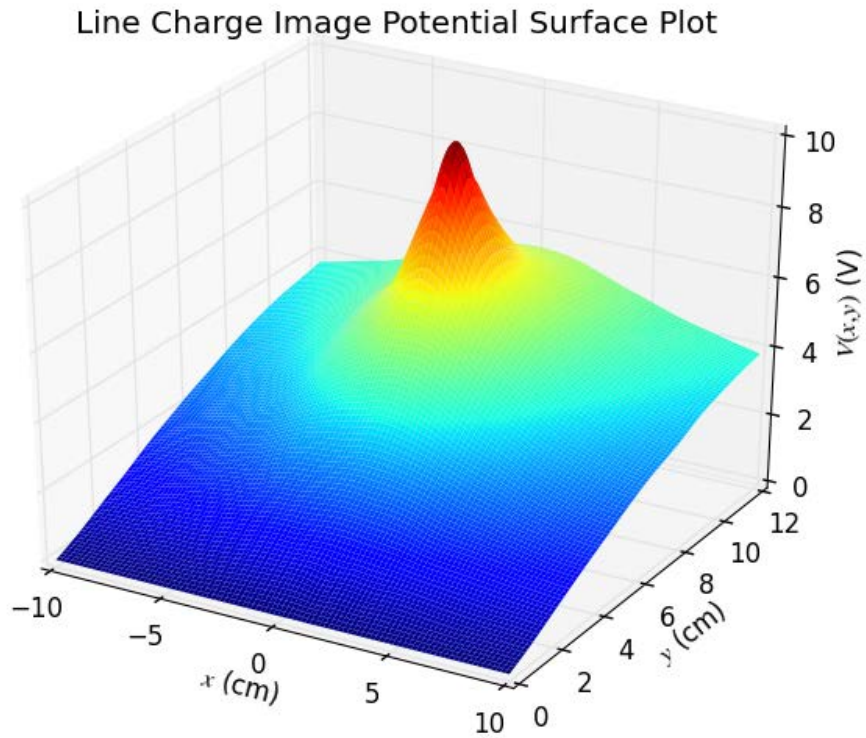


Figure 17 Line charge image surface plot. A circular equipotential of radius $R_0 = 0.5$ cm and potential $V_0 = 10.025$ V is placed a distance $y_0 = 8.0$ cm away from a grounded infinite conducting plane at $y = 0$. The color (as well as the height) indicates the magnitude of the potential, with blue being small potential and red being large potential.

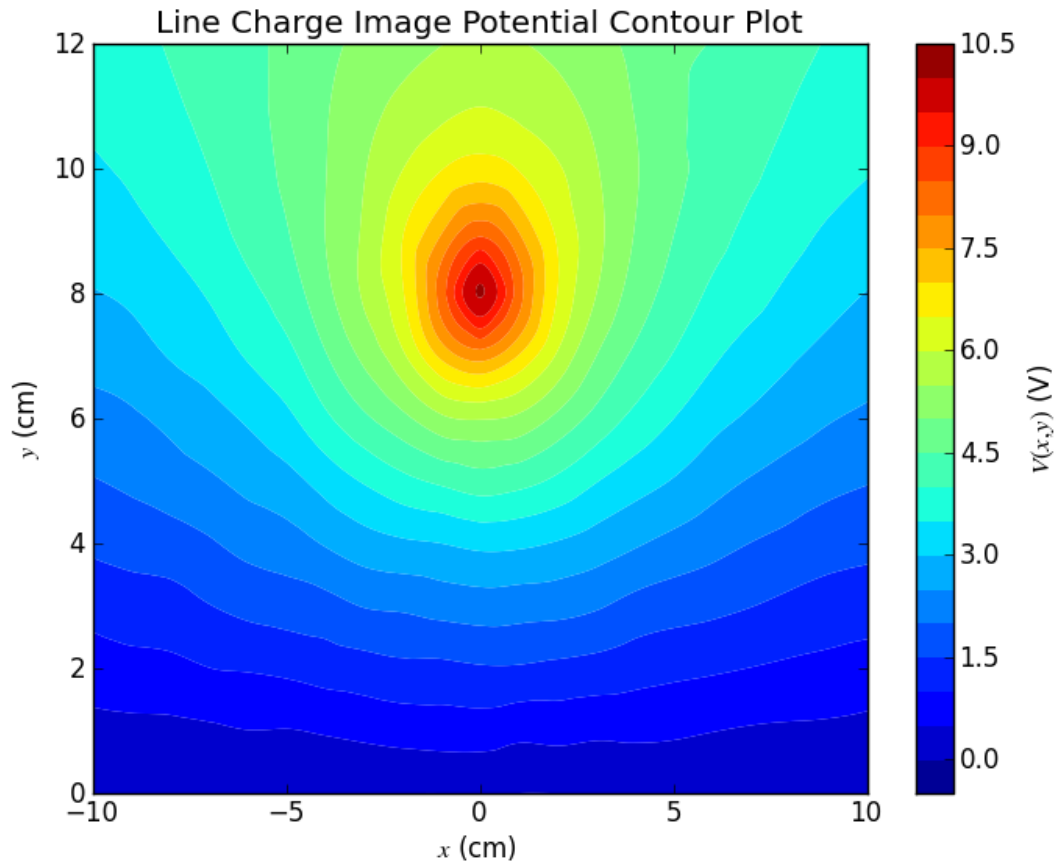


Figure 18 Line charge image contour plot. The 0.5 cm radius equipotential is centered at (0,8) cm and maintains constant potential of $V_0 = 10.025$ V. The grounded conducting plane is at $y = 0$. A total of 24 equipotential contour lines are plotted, with dense contours indicating rapid changes in potential.

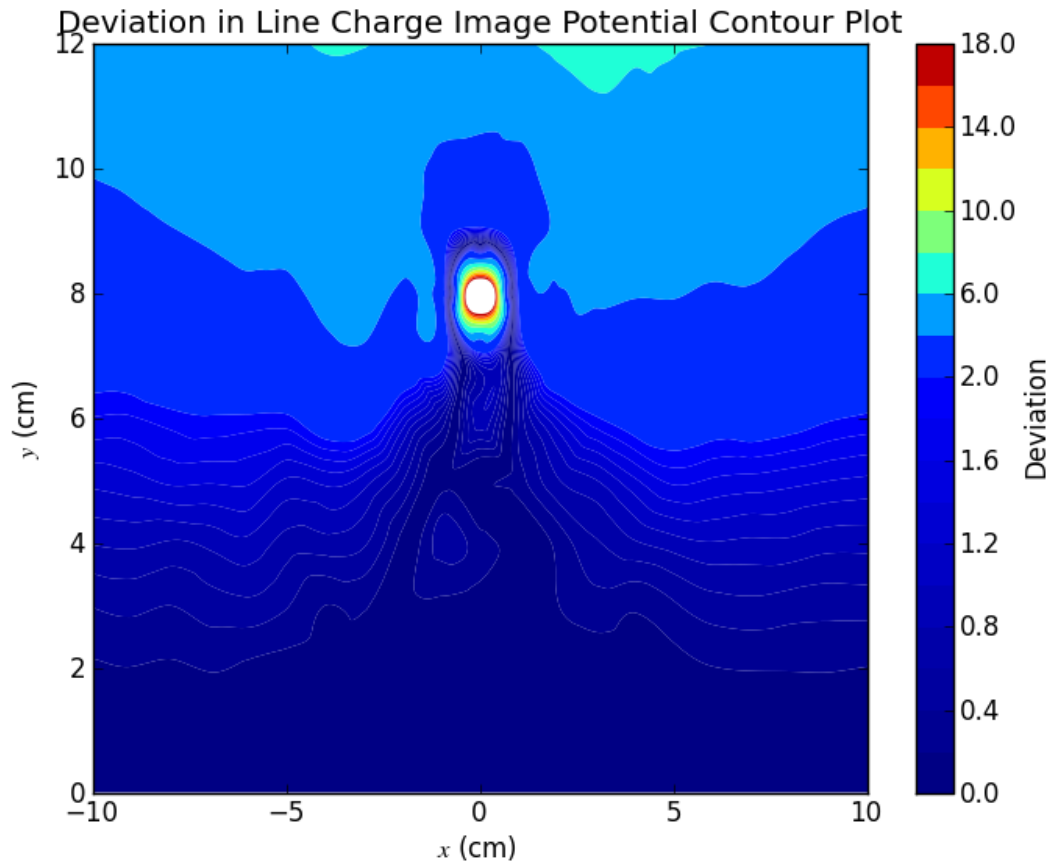


Figure 19 Relative deviation between theoretical and actual potentials for line charge image. The units are in number of deviations relative to the uncertainty in the potential of the theoretical model. The relative deviation between the theoretical model and measured potentials is typically less than 2 deviations (i.e. below $y = 8$ cm). Closer to the grounded plane ($y = 0$), the deviation is even less and falls within a single deviation.

Figures 20 and 21 show the numerical solutions to the line charge image configuration, and Figure 22 shows its deviation from the measured potentials. The largest absolute deviations occur near the peak around the equipotential, as shown by Figure 22.

Line Charge Image Finite Difference Potential Surface Plot

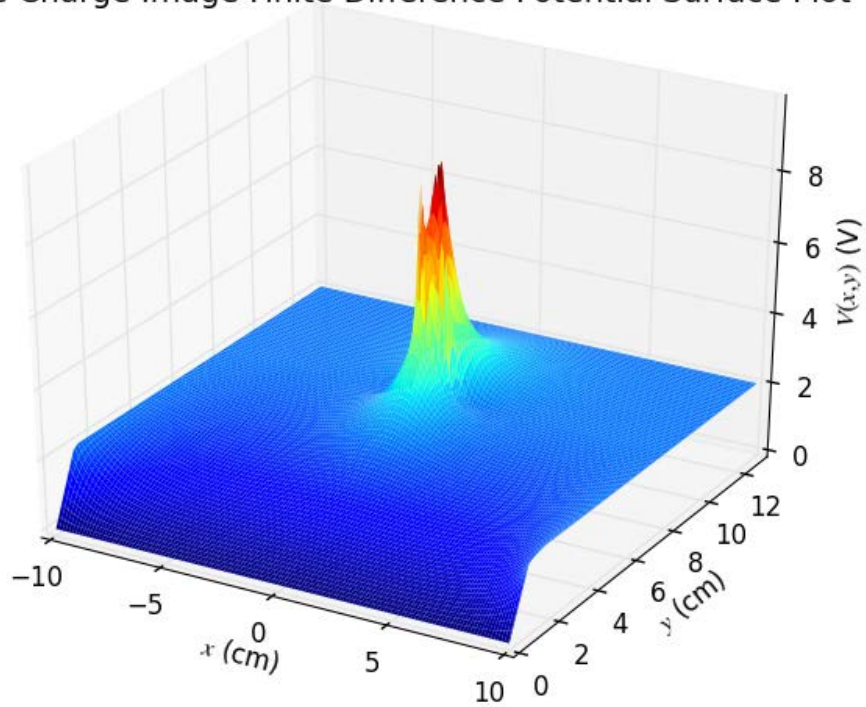


Figure 20 Surface plot of numerical solution to Laplace's equation for the line charge image. The solution area was initialized to a potential of $0.2V_0$ everywhere except for the peak, which was initialized at $2V_0$, where $V_0 = 10.025$ V. Where the grid mesh intersected the circular equipotential, the potential was fixed at V_0 , and the plane along $y = 0$ was fixed at 0.

Line Charge Image Finite Difference Potential Contour Plot

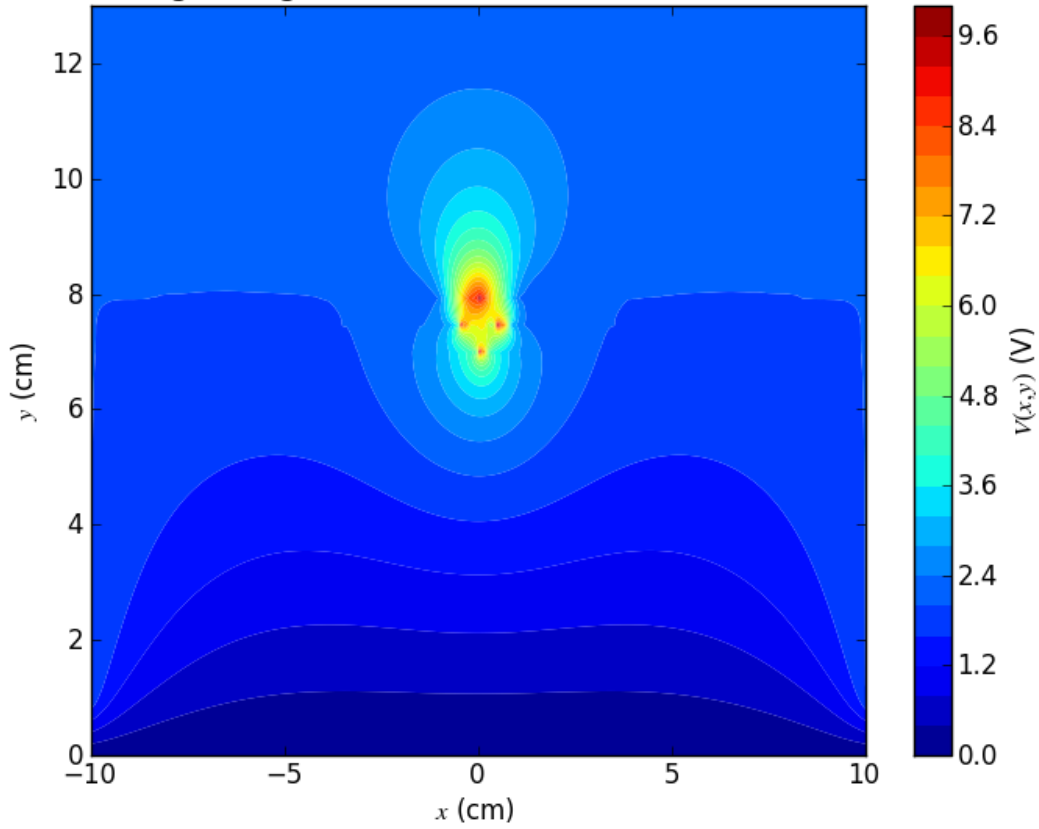


Figure 21 Contour plot of numerical solution to Laplace's equation for the line charge image. The solution area was initialized to a potential of $0.2V_0$ everywhere except for the peak, which was initialized at $2V_0$, where $V_0 = 10.025$ V. Where the grid mesh intersected the circular equipotential, the potential was fixed at V_0 , and the plane along $y = 0$ was fixed at 0.

Finite Difference Deviation in Line Charge Image Potential Contour Plot

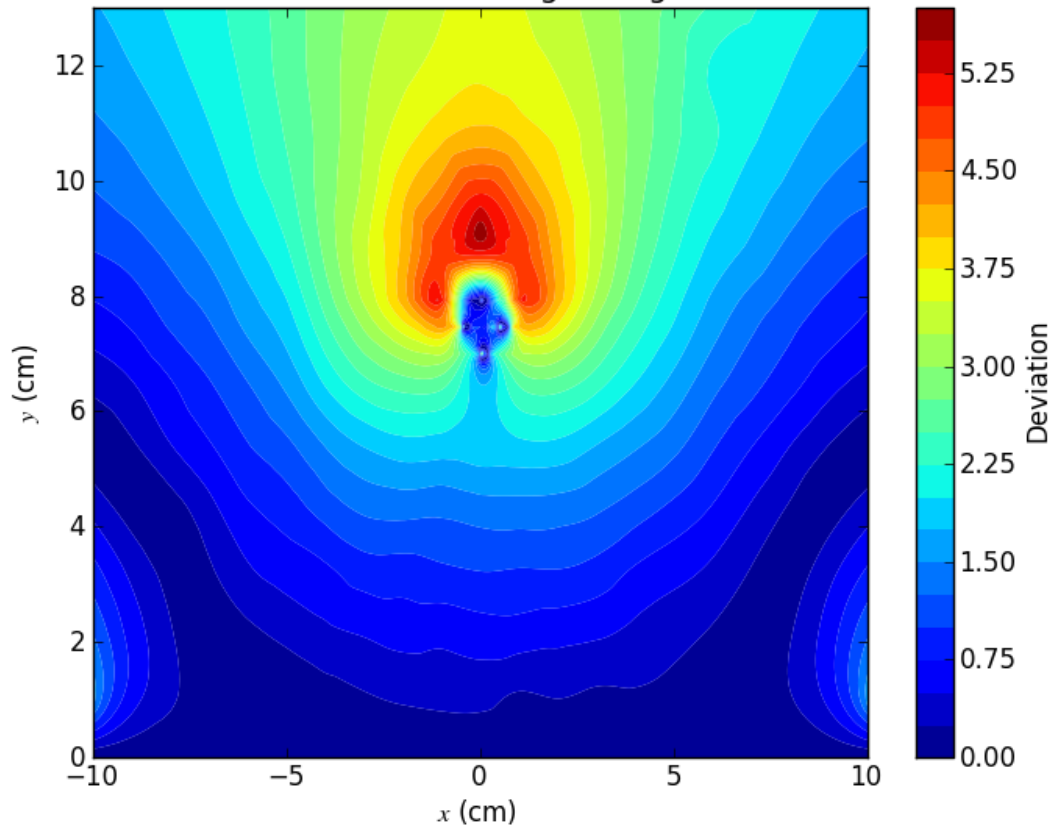


Figure 22 Absolute deviation between the numerical solution and measured potentials for the line charge image.

Parallel Plates with Insulator

Developing an analytic model or proper boundary conditions for a numerical solution could not be achieved due to uncertainties in the boundary conditions and insufficient information (such as the dielectric constant of the conductive medium). The potential within the insulator was prohibitively difficult to measure, as it decrease almost monotonically or oscillated around the grounded potential; only the potential at the boundary could be reliably determined. Thus, Figures 23 and 24 show the surface and contour plots of the potential as measured in the conductive medium and use grounded potential placeholder values in the insulator.

Insulating Box Potential Surface Plot

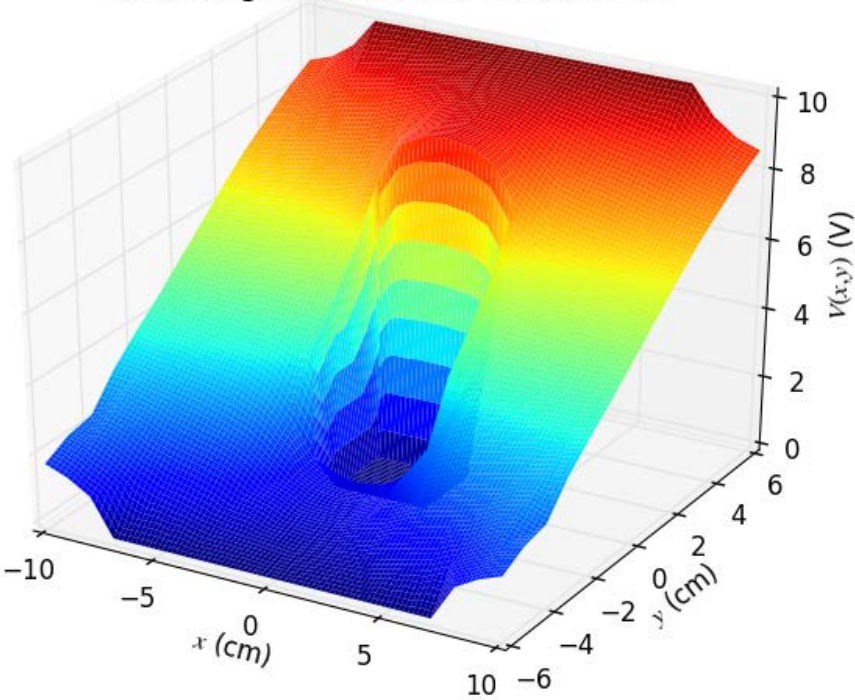


Figure 23 Insulating box surface plot. A box of dimensions 6 cm in the x direction and 4 cm in the y direction, centered at the origin, is depicted with zero potential inside since only the boundary potential could be reliably determined. The positive and negative electrodes have potentials of $V_0 = 10.025$ V and 0 V, respectively, and are located along the front and back edges ($y = \pm 6$ cm) with lengths of 12 cm. The color (as well as the height) indicates the magnitude of the potential, with blue being small potential and red being large potential.

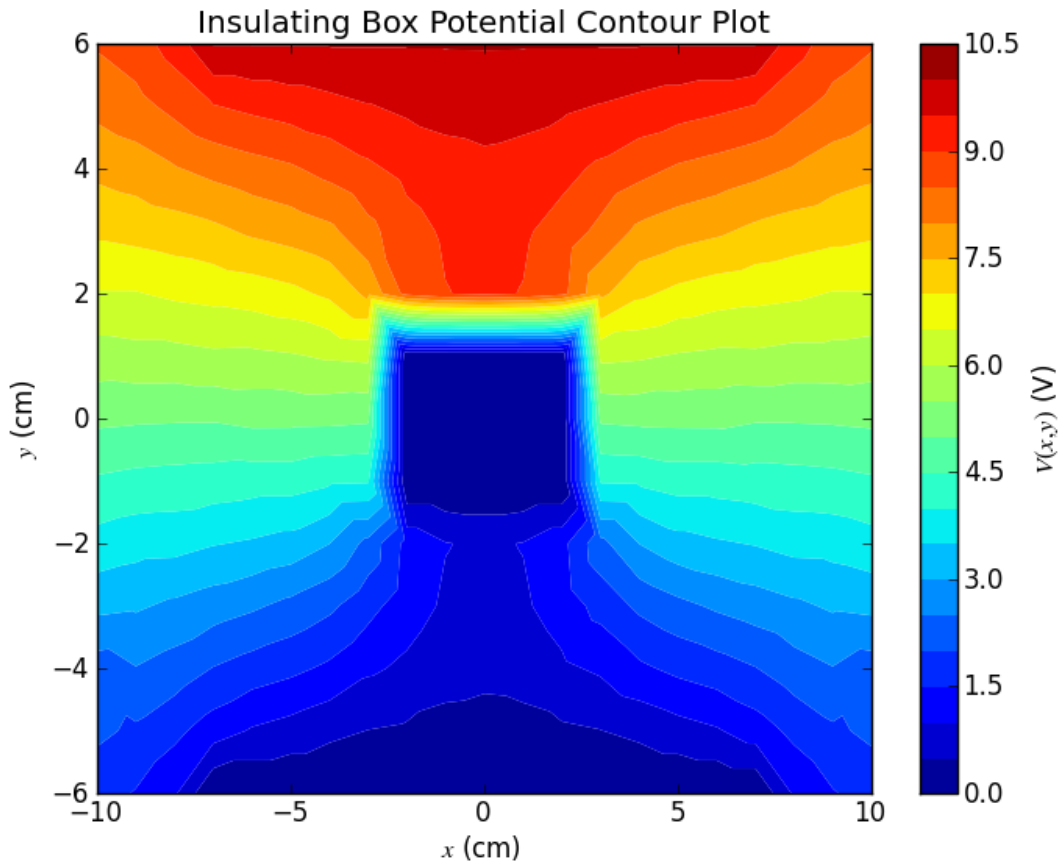


Figure 24 Insulating box contour plot. The insulating box spans from $-3 \text{ cm} < x < 3 \text{ cm}$ and $-2 \text{ cm} < y < 2 \text{ cm}$ with grounded potential placeholder values inside. The electrodes are at $y = \pm 6 \text{ cm}$ and have lengths of 12 cm. A total of 24 equipotential contour lines are plotted, with dense contours indicating rapid changes in potential.

Discussion and Conclusions

With the exception of the insulating box configuration, each of the configurations agreed within one to two deviations of the theoretical model potential in regions where the model was applicable. Qualitatively, the insulating box configuration behaved as expected, with smaller potential drops between the dielectric and the electrodes. The parallel plate capacitor had particularly large deviations on the edges and outside of the plates, where the theoretical model of an infinite parallel plate capacitor was no longer valid. A model (see e.g. [3,4]) which accounts for the strong electric fields on the edge of the plates would help to resolve this

discrepancy. The line charge image theoretical model also had very large deviations of 10 or more times its uncertainty from the measured value around the original circular equipotential. This is due to the theoretical model containing a pole that diverges logarithmically to infinity at the point where the line charge would be located. In the laboratory, we would not expect to measure such a diverging potential however, due to the finite dimensions of the experiment.

The numerical solutions to Laplace's equation were not quantitatively in close agreement with the measured values near sharp peaks and some of the boundaries, as can be seen in Figures 10, 16 and 22. Varying step sizes and initialization values have profound effects on the solution results and convergence rates. For example, the parallel plate capacitor was initialized to a value of $0.5V_0$, which did not change for most of the grid throughout the iteration. Using a larger step size would have propagated the boundary values more widely across the grid, resulting in a less uniform potential outside the plates. Additionally, the larger step sizes tended to converge faster, albeit with much less precision. Similarly, small step sizes would be better suited for computing values near sharp peaks, such as those in the cylindrical capacitor and line charge image configurations. However, computational memory limitations prevented smaller step sizes than were used. Thus, either the algorithm must be further optimized, additional computational resources obtained or the program rewritten in a more efficient computer language (e.g. C/C++).

Summary

The measured potentials agreed within one to two deviations of the theoretical model's potentials in most of the regions where the model was valid for each configuration. Improvements to the analytic model that account for edge effects and the finite dimensions of the geometry, although significantly more complicated, could decrease the deviation and increase the extent of the agreement between the theoretical and measured potentials. The potential within

the insulator could not be reliably determined, and a theoretical comparison could not be made due to insufficient information. However, the qualitative behavior of the potential around the insulator was in agreement with expectations: regions around the insulator reduced the steady currents and resulted smaller potential drops than if the insulator were absent. The numerical solutions to Laplace's equation agreed with the measured values in several regions of each configuration, but the solution and convergence rate depended heavily on the initialization of the method. Deviations of up to 100 percent were seen between the numerical solution and measured potential, with larger deviations observed near areas of rapid potential change. Further optimizations and experimentation with the initialization can be done to improve the relaxation method results.

References

- [1] Electric Fields Experiment Lab Manual.
- [2] D. J. Griffiths, *Introduction to Electrodynamics*, 3rd Ed. (Prentice Hall, New Jersey, 1999), p. 186, 288.
- [3] J. H. Jeans, *The Mathematical Theory of Electricity and Magnetism*, 2nd Ed. (Cambridge, 1911), p. 274-275.
- [4] W. Greiner, *Classical Electrodynamics*. (Springer, New York, 1998), p. 117-118.

Appendix: Solutions to Electrostatic Boundary Value Problems

Parallel Plate Capacitor

The infinite parallel plate capacitor with plates at $y = \pm \frac{a}{2}$, where a is the separation between the plates permits a solution of the form $V = V(y)$ by symmetry. Substituting this into Laplace's equation in Cartesian coordinates,

$$\nabla^2 V = 0 \Rightarrow \left(\frac{\partial^2}{\partial x^2} + \frac{\partial^2}{\partial y^2} + \frac{\partial^2}{\partial z^2} \right) V(y) = 0 \Rightarrow \frac{d^2 V(y)}{dy^2} = 0$$

which has a general solution $V(y) = Ay + B$. The boundary conditions require that

$$\begin{cases} V\left(-\frac{a}{2}\right) = V_1 \\ V\left(\frac{a}{2}\right) = V_0 \end{cases} \Rightarrow \begin{cases} -\frac{Aa}{2} + B = V_1 \\ \frac{Aa}{2} + B = V_0 \end{cases} \Rightarrow \begin{cases} B = \frac{1}{2}(V_0 + V_1) \\ A = \frac{V_0 - V_1}{a} \end{cases}$$

where V_1 and V_0 are the potentials of the lower and upper plates, respectively. So the voltage between the plates of an infinite parallel plate capacitor is given by Eq. 2a as

$$V(y) = \left(\frac{V_0 - V_1}{a}\right)y + \frac{1}{2}(V_0 + V_1)$$

Cylindrical Capacitor

The cylindrical capacitor consists of two concentric cylindrical conductors of radii $R_0 < R_1$ for the inner and outer cylinders, respectively. The inner conductor is held at potential V_0 , and the outer conductor is held at potential V_1 . Due to the cylindrical symmetry, the potential is independent of the azimuthal angle and depends only on the radial distance from the central axis: $V = V(r)$. Substituting this into Laplace's equation in cylindrical coordinates,

$$\nabla^2 V = 0 \Rightarrow \left(\frac{1}{r} \frac{\partial}{\partial r} \left(r \frac{\partial}{\partial r}\right) + \frac{1}{r^2} \frac{\partial^2}{\partial \phi^2} + \frac{\partial^2}{\partial z^2}\right) V(r) = 0 \Rightarrow \frac{1}{r} \frac{d}{dr} \left(r \frac{dV(r)}{dr}\right) = 0$$

The general solution is $V(r) = A + B \ln r$. In the region for $r < R_0$, the boundary conditions require that the potential be finite everywhere, so

$$\begin{cases} |V(0)| \neq \infty \\ V(R_0) = V_0 \end{cases} \Rightarrow \begin{cases} B = 0 \\ A = V_0 \end{cases}$$

In the region for $R_0 < r < R_1$, the boundary conditions are

$$\begin{cases} V(R_0) = V_0 \\ V(R_1) = V_1 \end{cases} \Rightarrow \begin{cases} A + B \ln R_0 = V_0 \\ A + B \ln R_1 = V_1 \end{cases} \Rightarrow \begin{cases} A = \frac{V_0 \ln R_1 - V_1 \ln R_0}{\ln\left(\frac{R_1}{R_0}\right)} \\ B = \frac{V_0 - V_1}{\ln\left(\frac{R_0}{R_1}\right)} \end{cases}$$

In the region for $r > R_1$, we again require that the potential be finite everywhere, so

$$\begin{cases} |V(\infty)| \neq \infty \\ V(R_1) = V_1 \end{cases} \Rightarrow \begin{cases} B = 0 \\ A = V_1 \end{cases}$$

Then the complete solution is

$$V(r) = \begin{cases} V_0, r < R_0 \\ \frac{V_0 \ln R_1 - V_1 \ln R_0}{\ln\left(\frac{R_1}{R_0}\right)} + \frac{V_0 - V_1}{\ln\left(\frac{R_0}{R_1}\right)} \ln r, R_0 < r < R_1 \\ V_1, r > R_1 \end{cases}$$

where $r = \sqrt{x^2 + y^2}$.

Line Charge Image

The potential for the configuration with a single line charge running parallel to an infinite, grounded conducting plane can be solved using the method of images by placing an image line charge of opposite charge density an equal distance away on the other side of the plane. Suppose that a line charge of charge density λ is a distance $y = a$ away from the conducting plane defined by $y = 0$ (i.e. the xz plane) and that the line charge runs parallel to the z axis at $x = 0$. Then an image line charge of charge density $-\lambda$ is placed at $y = -a$ parallel to the z axis at $x = 0$ as well. From cylindrical symmetry, Gauss's law can be used to calculate the electric field around a line charge:

$$\begin{aligned} \oint_S \mathbf{E} \cdot d\mathbf{A} &= \frac{Q}{\epsilon_0} \Rightarrow E(r) \oint_S \hat{\mathbf{r}} \cdot d\mathbf{A} = \frac{1}{\epsilon_0} \int_C \lambda(l') dl' \Rightarrow E(r) \oint_S dA = \frac{1}{\epsilon_0} \lambda L \Rightarrow E(r)(2\pi r L) = \frac{1}{\epsilon_0} \lambda L \\ \Rightarrow E(r) &= \frac{1}{2\pi\epsilon_0} \frac{\lambda}{r} \Rightarrow \mathbf{E}(\mathbf{r}) = E(r, \phi, z) = \frac{1}{2\pi\epsilon_0} \frac{\lambda}{r} \hat{\mathbf{r}} \end{aligned}$$

where $\hat{\mathbf{r}}$ points out from the line charge.

Then the potential is defined by $V(\mathbf{r}) = -\int_{\mathcal{O}}^{\mathbf{r}} \mathbf{E} \cdot d\mathbf{l}$ where $\mathcal{O} = (0,0,0)$, which corresponds to a radial displacement $r = a$ in cylindrical coordinates from the line charge. Thus,

$$V(\mathbf{r}) = -\int_{\mathcal{O}}^{\mathbf{r}} \mathbf{E}(\mathbf{l}') \cdot d\mathbf{l}' = -\int_a^r \frac{1}{2\pi\epsilon_0} \frac{\lambda}{r'} \hat{\mathbf{r}} \cdot dr' \hat{\mathbf{r}} = -\frac{\lambda}{2\pi\epsilon_0} [\ln|r'|]_a^r = \frac{\lambda}{2\pi\epsilon_0} \ln\left(\frac{a}{r}\right)$$

The radial distance from the line charges is given by $r_{\pm} = \|\mathbf{r} - \mathbf{r}_{\pm}\| = \sqrt{x^2 + (y \mp a)^2}$, and we use superposition to write the potential due to each line charge:

$$\begin{aligned} V(\mathbf{r}) = V(x, y, z) &= V_-(\mathbf{r}) + V_+(\mathbf{r}) = \frac{-\lambda}{2\pi\epsilon_0} \ln\left(\frac{a}{r_-}\right) + \frac{\lambda}{2\pi\epsilon_0} \ln\left(\frac{a}{r_+}\right) = \frac{\lambda}{2\pi\epsilon_0} \ln\left(\frac{r_-}{r_+}\right) \\ &= \frac{\lambda}{2\pi\epsilon_0} \ln\left(\frac{\sqrt{x^2 + (y + a)^2}}{\sqrt{x^2 + (y - a)^2}}\right) = \frac{\lambda}{4\pi\epsilon_0} \ln\left(\frac{x^2 + (y + a)^2}{x^2 + (y - a)^2}\right) \end{aligned}$$

The equipotential surfaces can then be found by setting $V(\mathbf{r}) = V_0$, where V_0 is the potential of that surface. The result is a function of x and y in terms of the parameters a , λ and V_0 that defines equipotential surfaces that are circular cylinders centered at $(0, a \coth(\frac{2\pi\epsilon_0 V_0}{\lambda}), z)$ for all $z \in \mathbb{R}$ and of radius $R = a \left| \operatorname{csch}\left(\frac{2\pi\epsilon_0 V_0}{\lambda}\right) \right|$.

Then defining a circular equipotential surface at voltage V_0 and of radius $R_0 = a \left| \operatorname{csch}\left(\frac{2\pi\epsilon_0 V_0}{\lambda}\right) \right|$ in the material at a distance $y_0 = a \coth\left(\frac{2\pi\epsilon_0 V_0}{\lambda}\right)$ away from the plane defines the corresponding line charge location $y = a$ and charge density λ . This permits the solution given above for the voltage in the region of interest. To find a and λ ,

$$\begin{cases} y_0 = a \coth\left(\frac{2\pi\epsilon_0 V_0}{\lambda}\right) \\ R_0 = a \left| \operatorname{csch}\left(\frac{2\pi\epsilon_0 V_0}{\lambda}\right) \right| \end{cases} \Rightarrow \begin{cases} a = \sqrt{y_0^2 - R_0^2} \\ \lambda = \frac{2\pi\epsilon_0 V_0}{a \operatorname{sech}\left(\frac{R_0}{y_0}\right)} \end{cases}$$

These solutions are valid provided that $0 < R_0 < y_0$. Thus, the potential in the region of interest is

$$V(\mathbf{r}) = V(x, y) = \frac{V_0}{2 \operatorname{asech}\left(\frac{R_0}{y_0}\right)} \ln\left(\frac{x^2 + (y + \sqrt{y_0^2 - R_0^2})^2}{x^2 + (y - \sqrt{y_0^2 - R_0^2})^2}\right)$$